

Effect of the shape of periodic forces and second periodic forces on horseshoe chaos in Duffing oscillator

V. Ravichandran^a, V. Chinnathambi^a, S. Rajasekar^{b,*}, Choy Heng Lai^c

^a*Department of Physics, Sri K.G.S. Arts College, Srivaikuntam 628 619, Tamilnadu, India*

^b*School of Physics, Bharathidasan University, Tiruchirappalli 620 024, Tamil Nadu, India*

^c*Department of Physics, National University of Singapore, Singapore 117542*

Abstract

The effect of the shape of six different periodic forces and second periodic forces on the onset of horseshoe chaos are studied both analytically and numerically in a Duffing oscillator. The external periodic forces considered are sine wave, square wave, symmetric saw-tooth wave, asymmetric saw-tooth wave, rectified sine wave, and modulus of sine wave. An analytical threshold condition for the onset of horseshoe chaos is obtained in the Duffing oscillator driven by various periodic forces using the Melnikov method. Melnikov threshold curve is drawn in a parameter space. For all the forces except modulus of sine wave, the onset of cross-well asymptotic chaos is observed just above the Melnikov threshold curve for onset of horseshoe chaos. For the modulus of sine wave long time transient motion followed by a periodic attractor is realized. The possibility of controlling of horseshoe and asymptotic chaos in the Duffing oscillator by an addition of second periodic force is then analyzed. Parametric regimes where suppression of horseshoe chaos occurs are predicted. Analytical prediction is demonstrated through direct numerical simulations. Starting from asymptotic chaos we show the recovery of periodic motion for a range of values of amplitude and phase of the second periodic force. Interestingly, suppression of chaos is found in the parametric regimes where the Melnikov function does not change sign.

Key words: Duffing oscillator, Melnikov method, horseshoe chaos, asymptotic chaos.

PACS: 05.45.+b

1. Introduction

The dynamics of nonlinear oscillators and circuits are very often studied with external force being of the form $f \sin \omega t$ or $f \cos \omega t$. Other forms of forces such as square wave, rectified sine wave, rectangular wave, etc. can be generated and applied to dynamical systems. The study of the effect of such periodic forces will be helpful to choose a suitable external drive in creating and controlling nonlinear behaviours. In recent years there are reports on the effect of different forces on certain nonlinear phenomena [1,2,3,4,5,6]. Analysis of features of a particular dynamics with various periodic forces and a detailed comparative study of effects induced by them will be of great use. It is also important to explore the utility and applicability of analytical methods such as multiple-scale perturbation theory and Melnikov method to the systems driven by periodic forces other than $f \sin \omega t$ and $f \cos \omega t$.

* Corresponding author. E-mail: srj.bdu@gmail.com; Fax +91 431 2407093; Phone +91 431 2407057

Motivated by the above, in the present paper we wish to study the occurrence of horseshoe chaos in Duffing oscillator driven by different periodic forces applying Melnikov analytical method. Recently, this method has been applied to study the Duffing and Duffing-van der Pol oscillators with different external perturbations [7,8,9,10,11,12,13,14]. The Melnikov method has also been applied to other nonlinear systems.

In the present paper, we consider the perturbed Duffing double-well oscillator

$$\dot{x} = y, \tag{1a}$$

$$\dot{y} = \omega_0^2 x - \beta x^3 + \epsilon [-\alpha y + F(t)], \tag{1b}$$

where α is the damping constant, ω_0^2 is the natural frequency, β is the stiffness constant which plays the role of nonlinear parameter, $F(t)$ is an external periodic force, ϵ is a small parameter, $\omega_0^2 > 0$, $\beta > 0$. We study the occurrence of horseshoe chaos with different periodic forces such as sine wave, square wave, symmetric saw-tooth wave, asymmetric saw-tooth wave, rectified sine wave and modulus of sine wave. In section 2, we obtain the Melnikov threshold condition for the transverse intersection of homoclinic orbits for the system (1) separately for each of the above periodic forces. In section 3, we plot the Melnikov threshold curve in the $(f - \omega)$ parameter space for all the forces where f and ω are the amplitude and frequency of the external periodic force. We verify the analytical prediction with the numerically calculated critical values of f at which transverse intersections of stable and unstable manifolds of the saddle occur. The Melnikov threshold value is also compared with the onset of asymptotic chaos wherever possible. Only for the modulus of sine wave long time transient motion instead of asymptotic chaos near the Melnikov threshold curve is found. We characterize the transient dynamics using the average transient time. In section 4, we consider the system (1) driven by two sine and modulus of sine forces and analyze the effect of the amplitude and phase of the second force. Starting from horseshoe chaos and asymptotic chaos we show the possibility of suppressing them. The control regions can be identified by the Melnikov method. Finally, we end up with conclusion in section 5.

2. Calculation of Melnikov function

The unperturbed part of the system (1) with $\epsilon=0$ has one saddle point $(x^*, y^*) = (0,0)$, and two center type fixed points, $(x^*, y^*) = (\pm\sqrt{\omega_0^2/\beta}, 0)$. The two homoclinic orbits connecting the saddle to itself are given by

$$W^\pm(x_h(t), y_h(t)) = \left(\pm\sqrt{2\omega_0^2/\beta} \operatorname{sech}\left(\sqrt{\omega_0^2} t\right), \mp\sqrt{2/\beta} \omega_0^2 \operatorname{sech}\left(\sqrt{\omega_0^2} t\right) \tanh\left(\sqrt{\omega_0^2} t\right) \right). \tag{2}$$

The Melnikov function $M(t_0)$ measures the distance between the stable manifold (W_s) and unstable manifold (W_u) of a saddle. When the two orbits are always separated then the sign of $M(t_0)$ always remains same. $M(t_0)$ oscillates when the orbits W_u and W_s intersect transversely (horseshoe dynamics). A zero of $M(t_0)$ corresponds to a tangential intersection. The occurrence of transverse intersections implies that the Poincaré map of the system has the so-called horseshoe chaos [1,15,16].

For the Duffing eq.(1), the Melnikov function is

$$M(t_0) = \int_{-\infty}^{\infty} y_h [-\alpha y_h + F(\tau + t_0)] d\tau. \tag{3}$$

In the following we calculate the Melnikov function for the system (1) with different periodic forces.

For the system (1) driven by the force $F(t) = f_{\sin} \sin \omega t$, the Melnikov integral (3) is worked out as

$$M_{\sin}^\pm(t_0) = A \pm f_{\sin} B \cos \omega t_0, \tag{4a}$$

where

$$A = -\frac{4\alpha}{3\beta} (\omega_0^2)^{3/2}, \quad B = \sqrt{2/\beta} \pi\omega \operatorname{sech}\left(\frac{\pi\omega}{2\sqrt{\omega_0^2}}\right). \quad (4b)$$

For the square wave $F(t) = F_{\text{sq}}(t + 2\pi/\omega) = f_{\text{sq}} \operatorname{sgn}(\sin\omega t)$ where $\operatorname{sgn}(y)$ is sign of y , using its Fourier series we obtain

$$M_{\text{sq}}^{\pm}(t_0) = A \pm f_{\text{sq}} \sum_{n=1}^{\infty} B_n \cos(2n-1)\omega t_0, \quad (5a)$$

where

$$B_n = \frac{4\sqrt{2}\omega}{\sqrt{\beta}} \operatorname{sech}\left(\frac{(2n-1)\pi\omega}{2\sqrt{\omega_0^2}}\right). \quad (5b)$$

For the symmetric saw-tooth wave of the form

$$F_{\text{sst}}(t) = F_{\text{sst}}(t + 2\pi/\omega) = \begin{cases} 4f_{\text{sst}}t/T, & 0 \leq t < \pi/2\omega \\ -4f_{\text{sst}}t/T + 2f_{\text{sst}}, & \pi/2\omega \leq t < 3\pi/2\omega \\ 4f_{\text{sst}}t/T - 4f_{\text{sst}}, & 3\pi/2\omega \leq t < 2\pi/\omega \end{cases} \quad (6)$$

the Melnikov function is

$$M_{\text{sst}}^{\pm}(t_0) = A \pm f_{\text{sst}} \sum_{n=1}^{\infty} B_n \cos(2n-1)\omega t_0, \quad (7a)$$

where

$$B_n = \frac{8\sqrt{2}\omega}{\pi\sqrt{\beta}} \frac{(-1)^{n+1}}{(2n-1)} \operatorname{sech}\left[\frac{(2n-1)\pi\omega}{2\sqrt{\omega_0^2}}\right]. \quad (7b)$$

For the asymmetric saw-tooth wave

$$F_{\text{ast}}(t) = F_{\text{ast}}(t + 2\pi/\omega) = \begin{cases} 2f_{\text{ast}}t/T, & 0 \leq t < \pi/\omega \\ 2f_{\text{ast}}t/T - 2f_{\text{ast}}, & \pi/\omega \leq t < 2\pi/\omega, \end{cases} \quad (8a)$$

we obtain

$$M_{\text{ast}}^{\pm}(t_0) = A \pm f_{\text{ast}} \sum_{n=1}^{\infty} B_n \cos n\omega t_0, \quad B_n = \frac{2\sqrt{2}\omega}{\sqrt{\beta}} (-1)^{n+1} \operatorname{sech}\left(\frac{n\pi\omega}{2\sqrt{\omega_0^2}}\right). \quad (8b)$$

For the rectified sine wave

$$F_{\text{rec}}(t) = F_{\text{rec}}(t + 2\pi/\omega) = \begin{cases} f_{\text{rec}} \sin\omega t, & 0 \leq t < \pi/\omega \\ 0, & \pi/\omega \leq t < 2\pi/\omega \end{cases} \quad (9)$$

we find

$$M_{\text{rec}}^{\pm}(t_0) = A \pm 2f_{\text{rec}} \sum_{n=1}^{\infty} B_n C_n \sin n\omega t_0, \quad (10a)$$

where

$$B_n = \frac{\sqrt{8}\omega\omega_0^2}{\pi\sqrt{\beta}} \frac{1}{\omega^2 - n^2}, \quad C_n = \int_{(2n-2)\pi/\omega}^{(2n-1)\pi/\omega} \operatorname{sech}\left(\sqrt{\omega_0^2}\tau\right) \tanh\left(\sqrt{\omega_0^2}\tau\right) \sin n\omega\tau d\tau. \quad (10b)$$

For the modulus of sine wave $F_{\text{msw}}(t) = F_{\text{msw}}(t + 2\pi/\omega) = f_{\text{msw}} \sin(\omega t/2)$, we find

$$M_{\text{msw}}^{\pm}(t_0) = A \pm f_{\text{msw}} \sum_{n=1}^{\infty} B_n \sin n\omega t_0, \quad (11a)$$

$$B_n = \frac{8\sqrt{2}\omega n^2}{(4n^2 - 1)\sqrt{\beta}} \operatorname{sech}\left(\frac{n\pi\omega}{2\sqrt{\omega_0^2}}\right). \quad (11b)$$

3. Horseshoe chaos and strange attractor

In this section, we compute the Melnikov threshold values for horseshoe chaos and compare it with numerical prediction. For the sine wave force the threshold condition for transverse intersections of stable manifolds (W_S^{\pm}) and unstable manifolds (W_U^{\pm}) is

$$|f_{\text{sin}}| \geq |f_M| = \frac{2\sqrt{2}\alpha(\omega_0^2)^{3/2}}{3\pi\omega\sqrt{\beta}} \cosh\left(\frac{\pi\omega}{2\sqrt{\omega_0^2}}\right). \quad (12)$$

For the other forces $M(t_0)$ is a convergent series. In these cases the threshold values of f can be determined numerically. For the rectified sine wave force C_n 's in eq.(10b) have to be calculated numerically. Throughout our study we fix the parameters in eq.(1) as $\alpha = 0.5$, $\beta = 1$, $\omega_0^2 = 1$ and $\omega = 1$. f_M can be calculated numerically as follows. For the forces other than sine and modulus of sine wave, we cannot write the sufficient condition for the existence of simple zeros of $M(t_0)$. Therefore, we identify the occurrence of homoclinic bifurcations by numerically measuring the time τ_M elapsed between two successive zeros of $M(t_0)$. τ_M is calculated for a range of amplitude of the external force. The value of f at which first time $M(t_0)$ changes sign and thereby giving finite τ_M is the Melnikov threshold value for homoclinic bifurcation.

Figure (1) shows the plot of f_M versus n , the number of terms in the summation, eq.(5a), for the square wave force. f_M converges to a constant value with increase in n . For $n > 10$, the variation in f_M is negligible. Similar result is found for the other forces also. In our numerical calculation of f_M we fix $n = 50$. Figure (2) shows the plot of the threshold curves for horseshoe chaos in the $(f - \omega)$ parameter plane. Below the threshold curve no transverse intersection of stable and unstable manifolds of the saddle occurs and above the threshold curve the transverse intersection of orbits of the saddle occurs. The threshold curves are nonintersecting. Smooth variation of f_M is found for all the forces considered in our study. The variation of f_M with ω is similar for all the periodic forces. Among the six forces, f_M is maximum for the asymmetric saw-tooth wave and is minimum for the square wave. Thus, onset of horseshoe chaos can be either delayed or advanced by an appropriate choice of periodic force.

We verify the analytical prediction by numerically computing the stable and unstable manifolds of the saddle. In fig.(3) we plotted the orbits of the saddle for two values of f – one for $f < f_M$ and another for $f > f_M$ for each of the forces. For clarity only part of the manifolds are shown. In the left side subplots, for $f = 0.2$, the stable and unstable orbits are well separated. In the right side subplots, for $f > f_M$, we can clearly notice transverse intersections of orbits at certain places. The critical values of f_M and f_{CWC} (at which onset of cross-well chaos occurs) for various forces are given in Table 1. The numerical result agrees well with the theoretical prediction.

For the system (1) driven by modulus of sine wave onset of cross-well chaos (asymptotic) is not observed near the Melnikov threshold value. However, transient motion followed by a long time periodic motion and hysteresis phenomenon are observed. Different paths are followed when f is increased from 0 to 0.5 and decreased from 0.5 to 0. Onset of jumping motion from left-well to right-well is found to occur at $f_h = 0.440547$. Long time transient motion is found for f values just below f_h . For a value of f , we calculated the transient time τ_T , the time taken to settle on the right-well attractor for a set of 900 initial conditions in the region $x \in [-0.9, -0.6]$, $\dot{x} \in [-0.2, 0]$. Then, average transient time τ is calculated for a range of values of f . Figure (4) shows the variation of τ as a function of $(f - f_c)$. τ is found to scale as $1.04166(f - f_c)^{-0.49}$.

Table 1

Critical values of f_M and f_{cwc} (the values of f at which cross-well chaos occur) for the Duffing eq.(1) for various forces with $\alpha = 0.5$, $\omega_0^2 = 1.0$, $\beta = 1.0$ and $\omega = 1.0$.

No. Force	f_M	f_{cwc}
1. Sine wave	0.3565	0.3833
2. Square wave	0.2745	0.2910
3. Symmetric saw-tooth wave	0.4629	0.4792
4. Asymmetric saw-tooth wave	0.7155	0.7326
5. Rectified sine wave	0.5026	0.5192
6. Modulus of sine wave	0.3985	— —

4. Effect of second periodic forces

In this section, we consider the problem of controlling of chaos by the addition of second weak periodic forces. We consider only the two forces, namely, sine wave and modulus of sine wave. The effect of other forces can also be studied.

In eq.(1) we choose $F(t) = f_{\sin} \sin \omega t + g_{\sin} \sin(\Omega t + \phi)$ where ϕ is the phase shift. Recently, Zambrano et al [17] studied suppression of chaos by the phase difference between the two external periodic forces. Wang et al [11] found the occurrence of strange non-chaotic attractor in the Duffing oscillator for a range of values of phase ϕ with the force $f \cos(\omega t) + g \cos(\Omega t + \phi(t))$.

For the system (1), the Melnikov function is

$$M_{\sin}^{\pm}(t_0) = A \pm B f_{\sin} \cos \omega t_0 \pm C g_{\sin} \cos(\Omega t_0 + \phi), \quad (13a)$$

where A and B are given by eq.(4b) and

$$C = \sqrt{2/\beta} \pi \Omega \operatorname{sech} \left(\frac{\pi \Omega}{2\sqrt{\omega_0^2}} \right). \quad (13b)$$

The choice $\Omega = \omega$ and $\phi = 0$ is trivial. For $\Omega \neq \omega$ a Melnikov condition similar to eq.(12) cannot be written for arbitrary values of ω and Ω . So, we numerically compute the time τ_M and identify the parametric regime where $1/\tau_M \approx 0$. In the absence of the second periodic force the horseshoe chaos is found to occur for $f=0.359$ and $\omega = 1$. We study the possibility of suppression of chaos by the addition of the second periodic force. Figure (5) shows the plot of $1/\tau_M$ against Ω for $g = 0.1$ and $\phi = 0$. In this figure $1/\tau_M$ is zero (that is, τ_M is infinity) only at $\Omega = 0.5$, 1.5 and $\Omega > 2.0$. This implies that horseshoe chaos does not occur for these three values of Ω . For other values of Ω , both $M^+(t_0)$ and $M^-(t_0)$ oscillate and hence $1/\tau_M$ are nonzero. These results are verified numerically.

Next, we study the effect of ϕ . For $\omega = \Omega$ and $\phi \neq 0$ (which gives $B = C$), the condition for $M(t_0)$ to change sign is given by

$$g_{\sin}^2 + 2f_{\sin} g_{\sin} \cos \phi + f_{\sin}^2 - (A^2/B^2) \geq 0. \quad (14)$$

The equality sign corresponds to tangential intersections of the orbits of saddle. We denote g_{\sin}^+ and g_{\sin}^- are the two roots of the eq.(14) with equality sign.

Figure (6) shows the plot of g_{\sin} versus ϕ for $\omega = \Omega = 1$, and $f = 0.359$. In the regions **a**, **b** and **c** enclosed by the continuous and dashed curves in fig.(6), the sign of $M(t_0)$ remains same and transverse intersection of orbits of the saddle does not occur. In the remaining region $M(t_0)$ oscillates and horseshoe chaos occurs. The above result is also confirmed by direct numerical simulation. We note that suppression of horseshoe chaos can be achieved for a range of values of ϕ , Ω and g_{\sin} . A striking result is that suppression of asymptotic chaotic motion is also found in the regions **a**, **b** and **c**. In fig.(7) bifurcation diagram and maximal Lyapunov exponent (λ) as a function of g_{\sin} are reported. For $\phi = 0.5$ the maximal Lyapunov exponent λ is found to be negative in the interval $g_{\sin} \in [-0.6077, 0.0108]$ while the interval of g in which suppression of horseshoe

chaos predicted by the Melnikov method is $[-0.6097, 0.0103]$. For $\phi = \pi$, suppression of asymptotic chaos is found in the interval $g_{\text{sin}} \in [-0.017, 0.735]$. The Melnikov method predicted interval of g for suppression of horseshoe chaos is $[-0.015, 0.735]$. Similar results are observed for various values of ϕ in the regions **a**, **b** and **c**.

For the Duffing oscillator driven by two modulus of sine wave

$$M_{\text{msw}}^{\pm}(t_0) = A \pm f_{\text{msw}} \sum_{n=1}^{\infty} B_n \sin(n\omega t_0) \pm g_{\text{msw}} \sum_{n=1}^{\infty} D_n \sin(n\Omega t_0 + \phi), \quad (15)$$

where A and B_n are given by the eqs.(4b) and (11) respectively and D_n is same as B_n except that ω in B_n is now replaced by Ω . We numerically compute the time τ_M and identify the parametric regions where $1/\tau_M \approx 0$. Figure (8) shows the plot of threshold values of g_{msw} versus ϕ for $\omega = \Omega = 1$, and $f_{\text{msw}} = 0.5$. In the regions **a**, **b** and **c** enclosed by the continuous and dashed curves in fig.(8), the sign of $M(t_0)$ remains same and transverse intersection of orbits of the saddle does not occur. In the remaining region $M(t_0)$ oscillates and horseshoe chaos occurs. The above result is also verified by numerical simulation. For example, fig.(9) shows the part of the stable and unstable orbits in the Poincaré map for two values of g_{msw} chosen outside and inside the region **b** for $\omega = \Omega = 1$, $\phi = \pi$ and $f = 0.5$. The threshold values of g_{msw} are $g_{\text{msw}}^+ = 0.615$ and $g_{\text{msw}}^- = 0.393$. When g_{msw} is varied from say -0.7 horseshoe chaos does not occur in the interval $g_{\text{msw}}^- < g < g_{\text{msw}}^+$. In fig.(9a) transverse intersections are seen for $g_{\text{msw}} = -0.1$. For $g_{\text{msw}} = 0.5$ (lying in the interval $[g_{\text{msw}}^-, g_{\text{msw}}^+]$) the stable and unstable orbits are well separated (fig.9b). Suppression of horseshoe chaos can be achieved for a range of values of ϕ , Ω and g_{msw} . The bifurcation diagram shows absence of cross-well chaos (asymptotic) near the Melnikov threshold value. However, long transient motion followed by a periodic motion and hysteresis phenomenon are observed.

5. Conclusion

In the present paper we have performed a numerical and analytical studies of homoclinic bifurcation in the Duffing oscillator driven by different periodic forces and addition of second periodic forces. Applying the Melnikov analytical method we obtained the threshold condition for onset of horseshoe chaos, that is, transverse intersections of stable and unstable branches of homoclinic orbits. For the modulus of sine wave instead of cross-well chaos a long time transient motion followed by a period- T solution is observed. Analytical prediction of horseshoe chaos is found to be in good agreement with numerical simulation for all the forces. Suppression of horseshoe chaos and asymptotic chaos are found for a range of amplitude of the second periodic force and phase shift between the two external forces. With the good agreement obtained between theoretical and numerical predictions we emphasize that the Melnikov analysis can be successfully used to predict the onset of chaos in the presence of weak periodic perturbations and also the effect of such perturbations on regular and chaotic dynamics.

In the Duffing oscillator driven by each of the different periodic forces considered in our study transverse intersection of left-well homoclinic orbits and transverse intersection of right-well homoclinic orbits occur at same critical values of, say, the amplitude f of the force. This is because in the absence of driving force and damping the potential is symmetric and the two homoclinic orbits connecting saddle to itself satisfy the relation $W^- = -W^+$. It is of interest to consider the situation where $W^- \neq \pm W^+$. In this case, it is possible to have onset horseshoe chaos (as well as asymptotic chaos) in the two wells at different threshold values. This will be analyzed in future.

Acknowledgements

The work reported here forms part of a Department of Science and Technology, Government of India research project of SR.

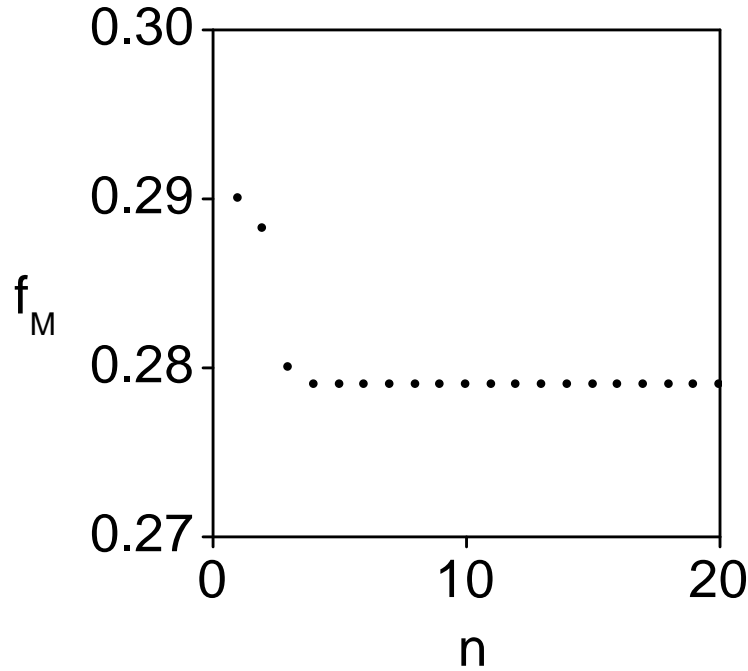


Fig. 1. f_M versus n , the number of terms in the summation in eq.(5a), for $\alpha = 0.5$, $\beta = 1$, $\omega_0^2 = 1$ and $\omega = 1$ when the system (1) is driven by the square wave force. Variation in f_M converges to a constant value with increase in n .

References

- [1] Chacon R, Control of Homoclinic Chaos by Weak Periodic Perturbations (World Scientific, Singapore, 2005).
- [2] Konishi K, Generating chaotic behaviours in an oscillator driven by periodic forces, Phys. Lett. A 2003; 320; 200-206.
- [3] Leung A.Y.T, Zengrong L, Suppressing chaos for some nonlinear oscillators, Int. J. Bifur. Chaos 2004; 14; 1455-1465.
- [4] Ge Z.M, Leu W.Y, Anticontrol of chaos of two degrees of freedom loud speaker system and synchronization of different order systems, Chaos, Solitons and Fractals 2004; 20; 503-521.
- [5] Lai Y.C, Liu Z, Nachman A, Zhu L, Suppression of jamming in excitable systems by aperiodic stochastic resonance, Int. J. Bifur. Chaos 2004; 14; 3519-3539.
- [6] Gandhimathi V.M, Rajasekar S, Kurths J, Effects of the shape of periodic forces on stochastic resonance, Int. J. Bifur. Chaos (2008, in press).
- [7] Nana Nbandjo B.R, Salissou Y, Wofo P, Active control with delay of catastrophic motion and horseshoe chaos in a single-well Duffing oscillator, Chaos, Solitons and Fractals 2005; 23; 809-816.
- [8] Tang Y, Yang F, Chen G, Zhou T, Classification of homoclinic tangencies for periodically perturbed systems, Chaos, Solitons and Fractals 2006; 28; 76-89.
- [9] Wang R, Deng J, Jing Z, Chaos control in Duffing system, Chaos, Solitons and Fractals 2006; 27; 249-257.
- [10] Balibrea F, Chacon R, Lopez M.A, Reshaping induced order-chaos routes in a damped driven Helmholtz oscillator, Chaos, Solitons and Fractals 2005; 24; 459-470.
- [11] Wang X, Lai Y.C, Lai C.H, Effect of resonant-frequency mismatch in attractors, Chaos 2006; 16; 023127.
- [12] Yang J, Feng W, Jing Z, Complex dynamics in Josephson system with two external forcing terms, Chaos, Solitons and Fractals 2006; 30; 235-256.
- [13] Jing Z, Yang Z, Jiang T, Complex dynamics in Duffing-van der Pol oscillators, Chaos, Solitons and Fractals 2006; 27; 722-747.
- [14] Gao H, Chen G, Global and local control of homoclinic and heteroclinic bifurcations, Int. J. Bifur. Chaos 2005; 15; 2411-2432.
- [15] Guckenheimer J, Holmes P, Dynamical Systems and Bifurcations of Vector Fields (Springer, New York, 1990).
- [16] Wiggins S, Introduction to Applied Nonlinear Dynamical Systems and Chaos (Springer, New York, 1990).
- [17] Zambrano S, Allaria E, Brugioni S, Leyva I, Meucci R, Sanjuan M.A.F, Arecchi F.T, Numerical and experimental exploration of phase control of chaos, Chaos 2006; 16; 013111.

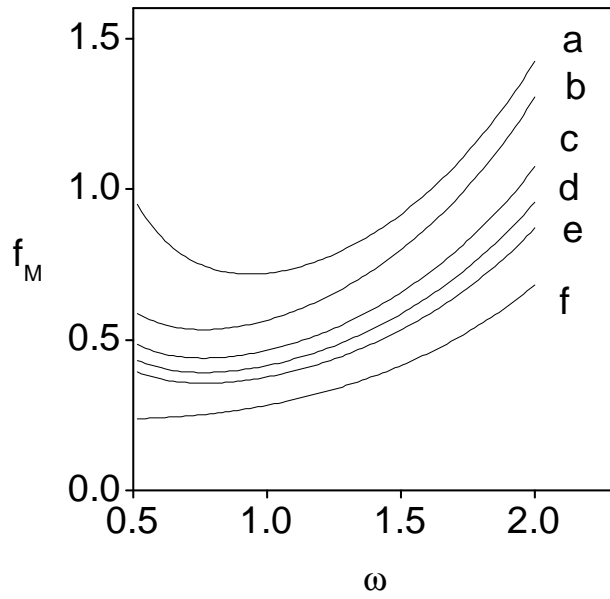


Fig. 2. Melnikov threshold curves for horseshoe chaos in the $(f-\omega)$ plane for the system (1) driven by the forces (a) asymmetric saw-tooth wave, (b) rectified sine wave, (c) symmetric saw-tooth wave, (d) modulus of sine wave, (e) sine wave and (f) square wave. The values of the parameters in eq.(1) are $\alpha = 0.5$, $\beta = 1$ and $\omega_0^2 = 1$.

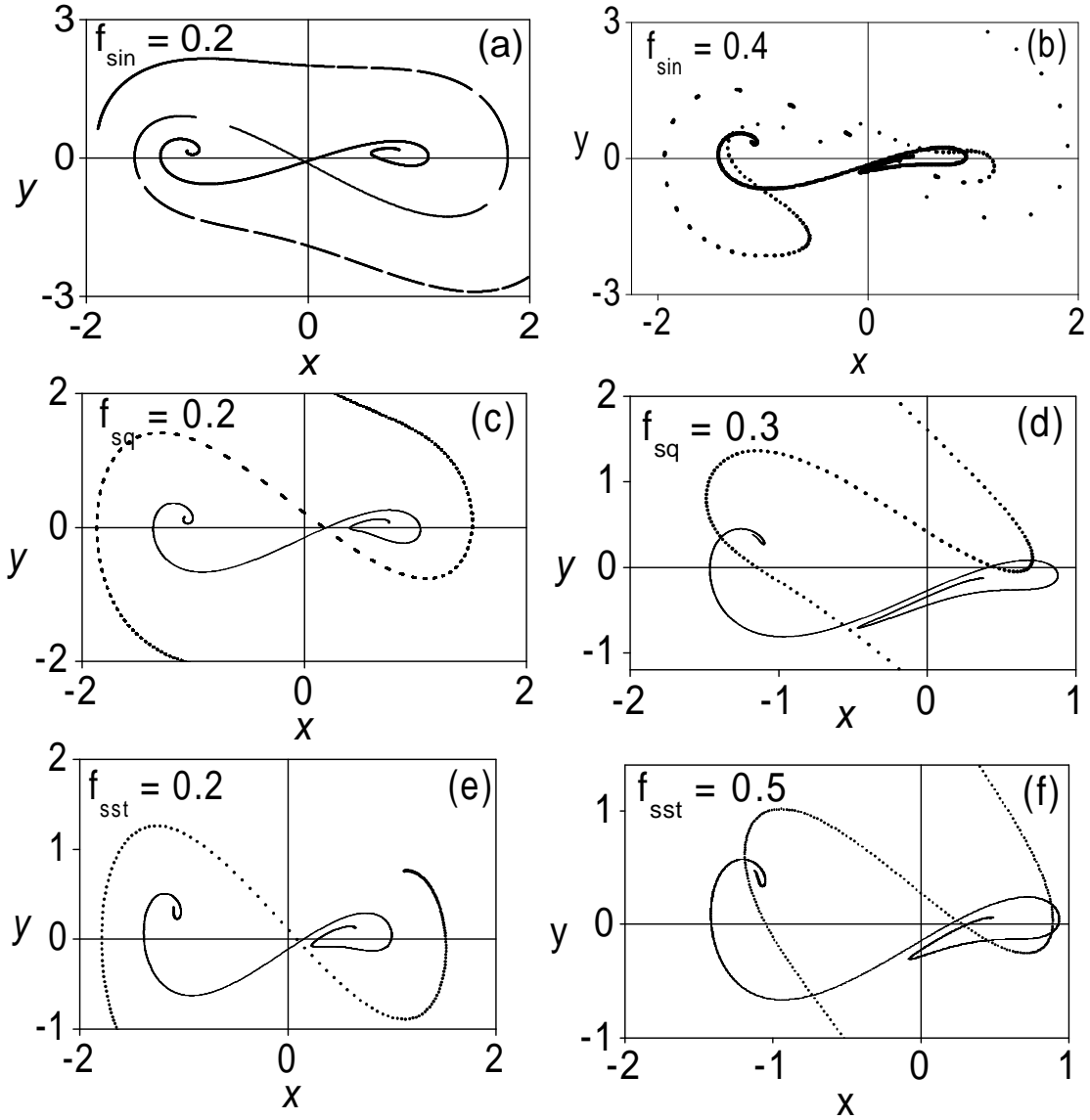


Fig. 3. Numerically computed stable and unstable manifolds of the saddle fixed point of the system (1). The system is driven by (a-b) sine wave, (c-d) square wave, (e-f) symmetric saw-tooth wave, (g-h) asymmetric saw-tooth wave, (i-j) rectified sine wave and (k-l) modulus of sine wave. The other parameters are $\alpha = 0.5$, $\beta = 1$, $\omega_0^2 = 1$ and $\omega = 1$. Left side subplots are for $f < f_M$ while the right side subplots are for $f > f_M$.

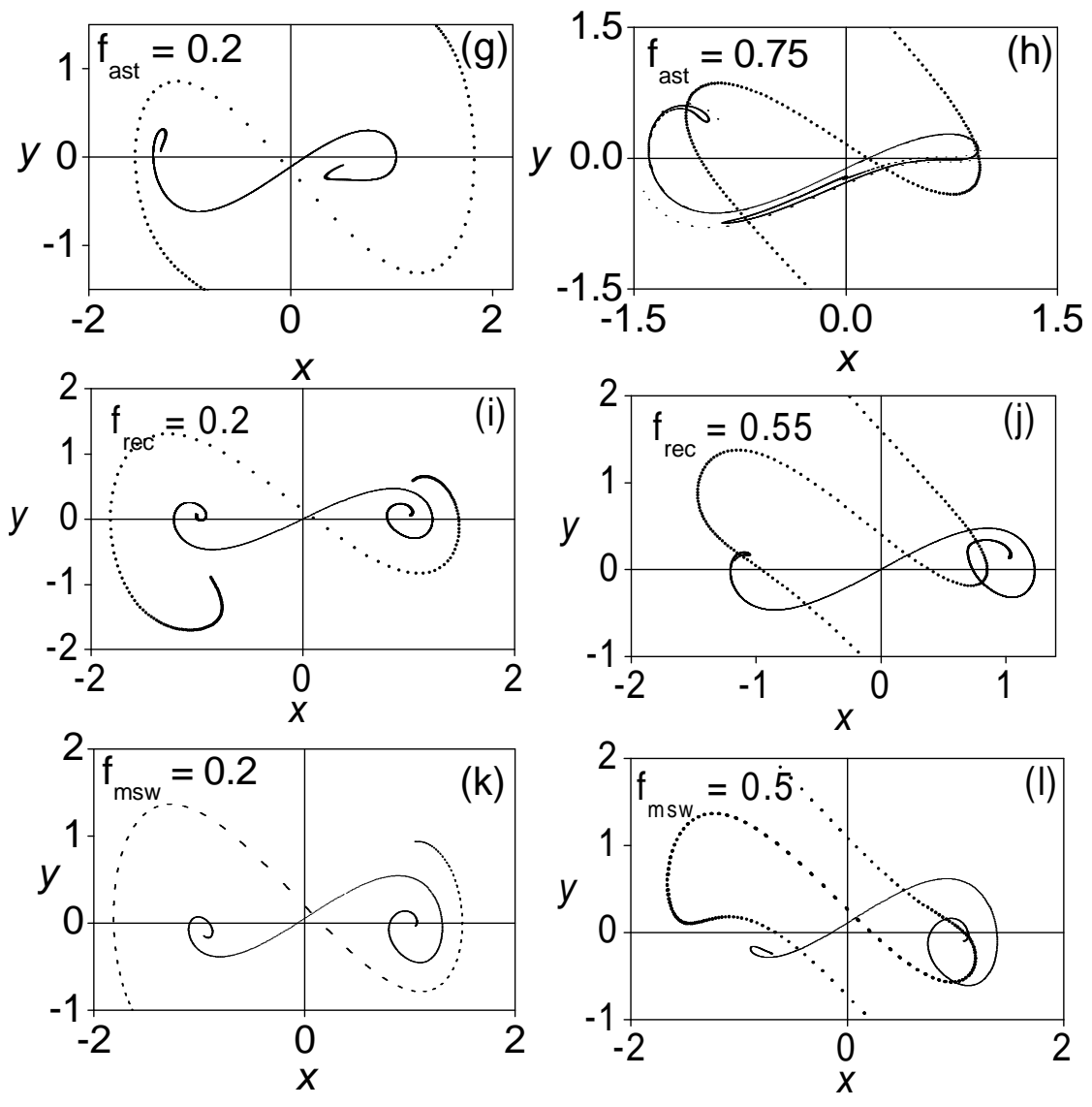


Fig. 3. continued...

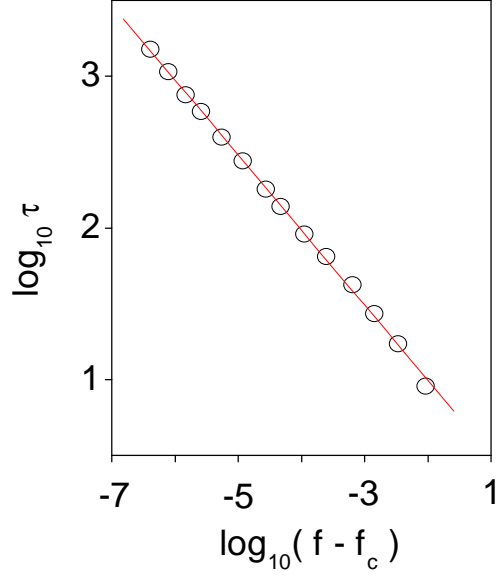


Fig. 4. Variation of τ as a function of $(f - f_c)$. τ is found to scale as $1.04166 (f - f_c)^{-0.49}$.

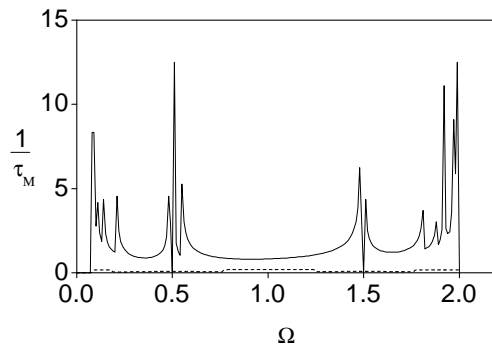


Fig. 5. $1/\tau_M$ versus Ω for the system (1) with $F(t) = f_{\text{sin}} \sin \omega t + g_{\text{sin}} \sin(\Omega t + \phi)$, $g_{\text{sin}} = 0.1$, $f_{\text{sin}} = 0.359$, $\alpha = 0.5$, $\beta = 1$, $\omega_0^2 = 1$, $\omega = 1$ and $\phi = 0$. Continuous curve corresponds to positive sign while dashed curve corresponds to negative sign in eq.(13).

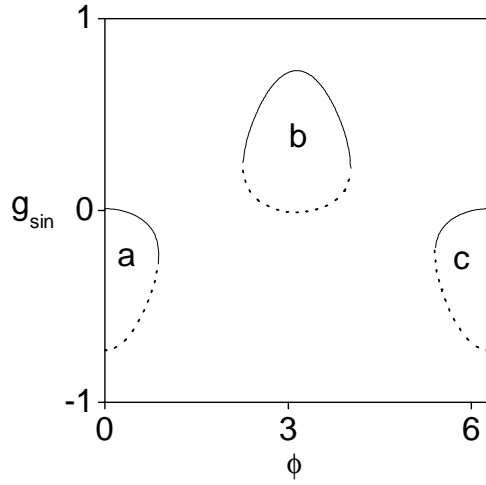


Fig. 6. Graph of the roots of g_{\sin}^{\pm} of eq.(14) with equality sign. Horseshoe dynamics does not occur in the regions **a**, **b**, and **c** enclosed by the curves. Continuous and dashed curves represent g_{\sin}^+ and g_{\sin}^- respectively. The other parameters are $f_{\sin} = 0.359$, $\alpha = 0.5$, $\beta = 1$, $\omega = \Omega = 1$ and $\omega_0^2 = 1$.

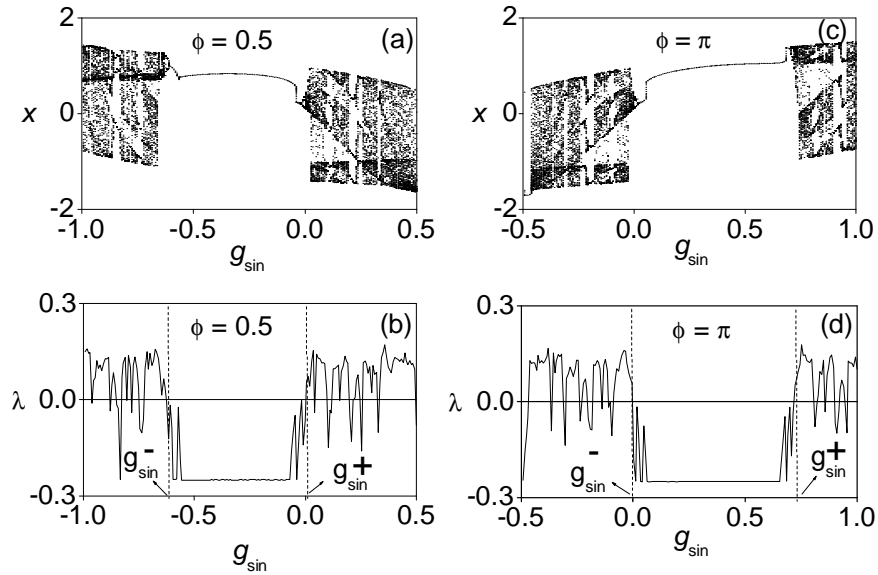


Fig. 7. Bifurcation diagrams and the corresponding maximal Lyapunov exponent illustrating the effect of ϕ and g on chaotic dynamics. The parameters are fixed as $\alpha = 0.5$, $\beta = 1$, $\omega_0^2 = 1$, $\omega = \Omega = 1$, $f_{\sin} = 0.359$. For $g_{\sin} = 0$ the system exhibits chaotic motion.

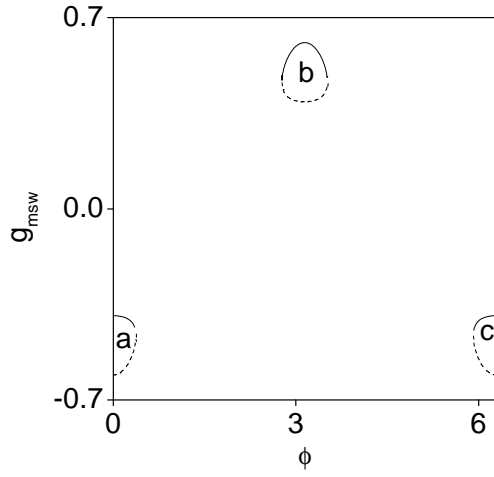


Fig. 8. Graph of g_{msw}^{\pm} . Horseshoe dynamics does not occur in the regions **a**, **b**, and **c** enclosed by the curves. The other parameters are $f_{\text{msw}} = 0.5$, $\alpha = 0.5$, $\beta = 1$, $\omega = \Omega = 1.0$ and $\omega_0^2 = 1$.

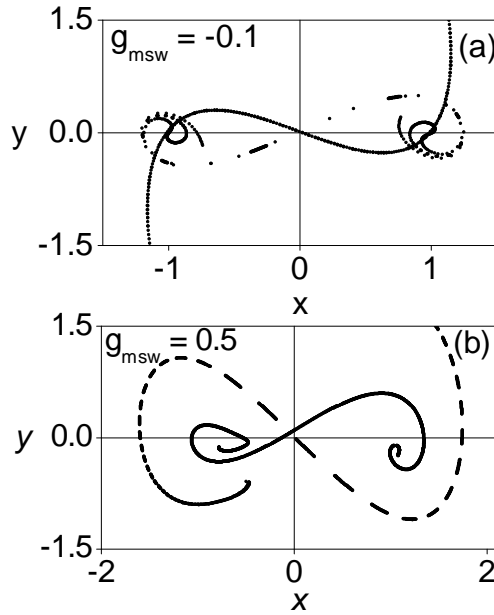


Fig. 9. Numerically computed part of perturbed homoclinic orbits for (a) $g_{\text{msw}} = -0.1$ and (b) $g_{\text{msw}} = 0.5$. The other parameters are fixed at $\alpha = 0.5$, $\beta = 1$, $\omega_0^2 = 1$, $\phi = \pi$, $\Omega = \omega = 1$ and $f_{\text{msw}} = 0.5$.